Supporting information

Rational Design of Redox Active Metal Organic Frameworks for Mediated Electron Transfer of Enzyme

Muhammad Rezki [a], Md Motaher Hossain[a], Thomas Kouyou Savage[b], Yoshihide Tokunou[c,d], and Seiya Tsujimura[e,*]

[a.]Graduate School of Pure and Applied Science, University of Tsukuba, 1-1-1, Tennodai, Ibaraki 305-5358, Japan
[b.]Degree Programs in Life and Earth Sciences, University of Tsukuba, 1-1-1, Tennodai, Ibaraki 305-8577, Japan
[c.]Department of Life and Environmental Sciences, University of Tsukuba, 1-1-1 Tennodai, Ibaraki 305-8577, Japan
[d.]Research Center for Macromolecules and Biomaterials, National Institute for Materials Science, 1-1 Namiki 305-0044, Ibaraki, Japan
[e.]Department of Material Science, Institute of Pure and Applied Science, University of Tsukuba, 1-1-1, Tennodai, Ibaraki 305-5358, Japan.
* Email: seiya@ims.tsukuba.ac.jp

Supplementary S1: Experimental section

Chemicals

2-Methyl imidazole (MeIm), cobalt nitrate hexahydrate (99.5%), zinc nitrate hexahydrate (99.9%), copper (II) nitrate trihydrate (99.9%), iron (III) Chloride Hexahydrate (99%), Benzene-1,4-dicarboxylic acid (BDC), triethylamine, polyvinylpyrrolidone K 90 (PVP), genipin, were purchased from Wako Fujifilm, Japan. Thin multiwalled carbon nano tubes (CNT) (Nanocyl 3100) were purchased from Nanocyl SA (Belgium). 1,2-Naphtoquione-4-sulfonate sodium salt (NQSO) was purchased from Sigma Aldrich. Chitosan (200-600Mpa), 1,2-naphthoquinone, Sodium anthraquinone-2-sulfonate, were purchased from Tokyo Chemical Co. Ltd., Japan. Ketjen Black (KB) (EC 600JD) and magnesium templated porous carbon (MgOC) (100 nm pores) were purchased from CNovel, Japan. FADGDH was purchased from Ikeda Tohka Industries, Japan. All chemicals were used without further purification. LOx was donated by the Institute of Physical and Chemical Research (RIKEN, Japan).

Synthesis of Co-MeIm

2-Methyl imidazole (5.675 g) was dissolved in 25 mL of methanol (ligand solution), subsequently 0.3 g of Cobalt nitrate hexahydrate in 3 mL methanol was poured into the ligand solution under stirring for 30 minutes. After that the mixture was kept at room temperature (25^{o}C) for overnight, followed by centrifugation process to collect the precipitate (200.000 x g, 2 min). The obtained precipitate was then washed three times with methanol and dry at 60C for overnight. Finally, by mechanically grinding the purple Co-MeIm powder was obtained.

Synthesis of CNT/Co-MeIm and CNT/Zn-MeIm

CNTs (60 mg) were dispersed in 10 mL of methanol containing PVP (0.24 mg) by sonication for 15 min, followed by 30 min of stirring. The CNTs were then washed and re-dispersed in methanol (5 mL). 2-Methyl imidazole (5.675 g) was dissolved in methanol (25 mL) and the CNT dispersion was added to this solution while stirring. Cobalt nitrate hexahydrate (0.3 g) was dissolved in methanol (3 mL) and then poured into the solution containing 2-methyl imidazole and CNTs. After incubation overnight, the CNT/Co-MeIm mixture was centrifuged. The precipitate was collected, washed three times with methanol, and dried at 60 °C overnight. Finally, the fine CNT/Co-MeIm powder was obtained by mechanical grinding

For the CNT/Zn-MeIm synthesis, zinc nitrate hexahydrate was used instead of cobalt. For the synthesis of MgOC/Co-MeIm and KB/Co-MeIm, MgOC and KB were used instead of CNT. The synthetic procedure was otherwise analogous

Synthesis of CNT/Fe-BDC and CNT/Cu-BDC

CNT/Fe-BDC was synthesized according to the reported literature[1,2] with hand full modification, CNTs (60 mg) were dispersed in 5 mL of DMF by sonication for 15 min. BDC ligand (0.412 g) was dissolved in 20 mL of DMF. The CNT dispersion was then poured to the ligand solution under stirring. Iron Chloride (0.7 g) was dissolved in DMF (3 mL) and then poured into the solution containing BDC and CNTs under stirring. The mixture was then transferred into Teflon lined autoclave to perform solvothermal treatment at 115oC for 24h. after that the precipitate was collected and washed several times with DMF and followed by drying process at 90C under vacuum.

CNT/Cu-BDC was synthesized according to the reported literature[3] with hand full modification, CNTs (60 mg) were dispersed in 5 mL of DMF by sonication for 15 min. BDC ligand (0.412 g) was dissolved in 20 mL of DMF. The CNT dispersion was then poured to the ligand solution under stirring. 100 μL of triethyl amine then was added to promote the deprotonation of BDC ligand. Cooper nitrate (0.7 g) was dissolved in DMF (3 mL) and then poured into the solution containing BDC and CNTs under stirring. The mixture was then agitated at room temperature for 24h to allow the precipitation process. after that the precipitate was collected and washed several times with DMF and followed by drying process at 90C under vacuum.

NQSO ligand substitution

The material powder (Co-MeIm, CNT/Co-MeIm, CNT, CNT/Zn-MeIm, CNT/Fe-BDC, CNT/Cu-BDC, MgOC/Co-MeIm or KB/Co-MeIm) was heated at 90–100°C under vacuum for 24 h. Next, 20 mg of treated material was dispersed in an aqueous solution of 1,2-naphtoquinone-4-sulfonate (NQSO) (320 μM, 20 mL). This was followed by sonication for 2-5 min, then incubation for 24 h. The Material-NQSO mixture was centrifuged (200.000 x g, 2 min). The precipitate was collected and washed five times with water. The obtained material-NQSO precipitate was re-dispersed in water (1 mL). For other redox active MOF including CNT/Co-MeIm-14NQSO, and CNT/Co-MeIm-AQSO, similar procedures were used except the replacement of NQSO with the desired

redox molecules. For NQ, 1,2-naphtoquinone was first dissolved in acetonitrile and then diluted with water to obtain 320 µM final concentration in 20 mL.

Electrode preparation

The dispersion of the material (20 mg/mL) was sonicated to obtain a homogenous ink suspension, which was drop-cast onto the clean glassy carbon electrode (GCE) surface. After drying, a hydrogel mixture containing chitosan (1 wt. % in 1% acetic acid), genipin (30 mg in 1 mL ethanol), and FADGDH or LOx, in a 10:5:20 µL ratio was coated onto the modified electrode surface. The modified electrode was immediately incubated at 4 °C for 3 d. The electrode was then immersed in water and phosphate buffered saline (PBS) for several hours to remove the uncross-linked reagents. When not in use, the electrode was stored at 4 °C with immersion in PBS.

Characterization

Scanning electron microscopy (SEM) was performed using a Hitachi High-Tech instrument (SU-8020). Fourier transform infrared (FTIR) spectroscopy was performed by the KBR method using a Jasco FT/IR-4X. The XRD characterization was carried out using Cu Kα source, the database for the ZIF was referred to from the crystallographic open data base (COD-7236367)[4]. The N_2 adsorption–desorption isotherm of the sample was evaluated using BELSORP-max-11-N-VP at 77 K. The XPS characterization was evaluated using JEOL (JPS-9010TR) with Mg K α as the X-ray source. All electrochemical characterization experiments were conducted using a 3-electrode system with Ag/AgCl as the reference electrode, a platinum wire as the counter electrode, and glassy carbon as the working electrode. A Palmsens potentiostat was used for the short-term experiment, whereas the potentiostat/galvanostat HA-151B was used for the long-term experiment. Phosphate buffer saline (0.1 M) was used as electrolyte.

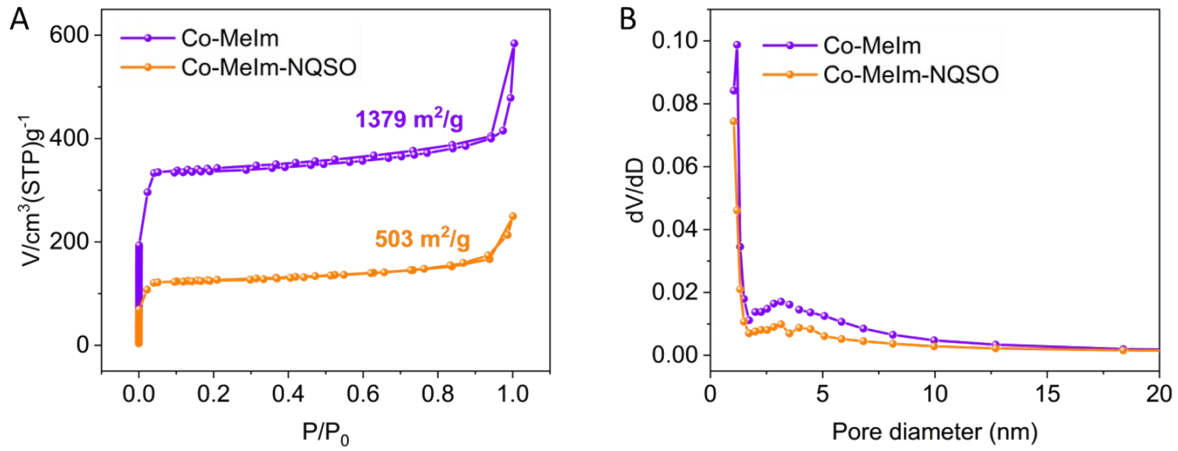

Fig. S1. A. N_2 absorption desorption isotherm curve, and B. Pore distribution of Co-MeIm and Co-MeIm-NQSO

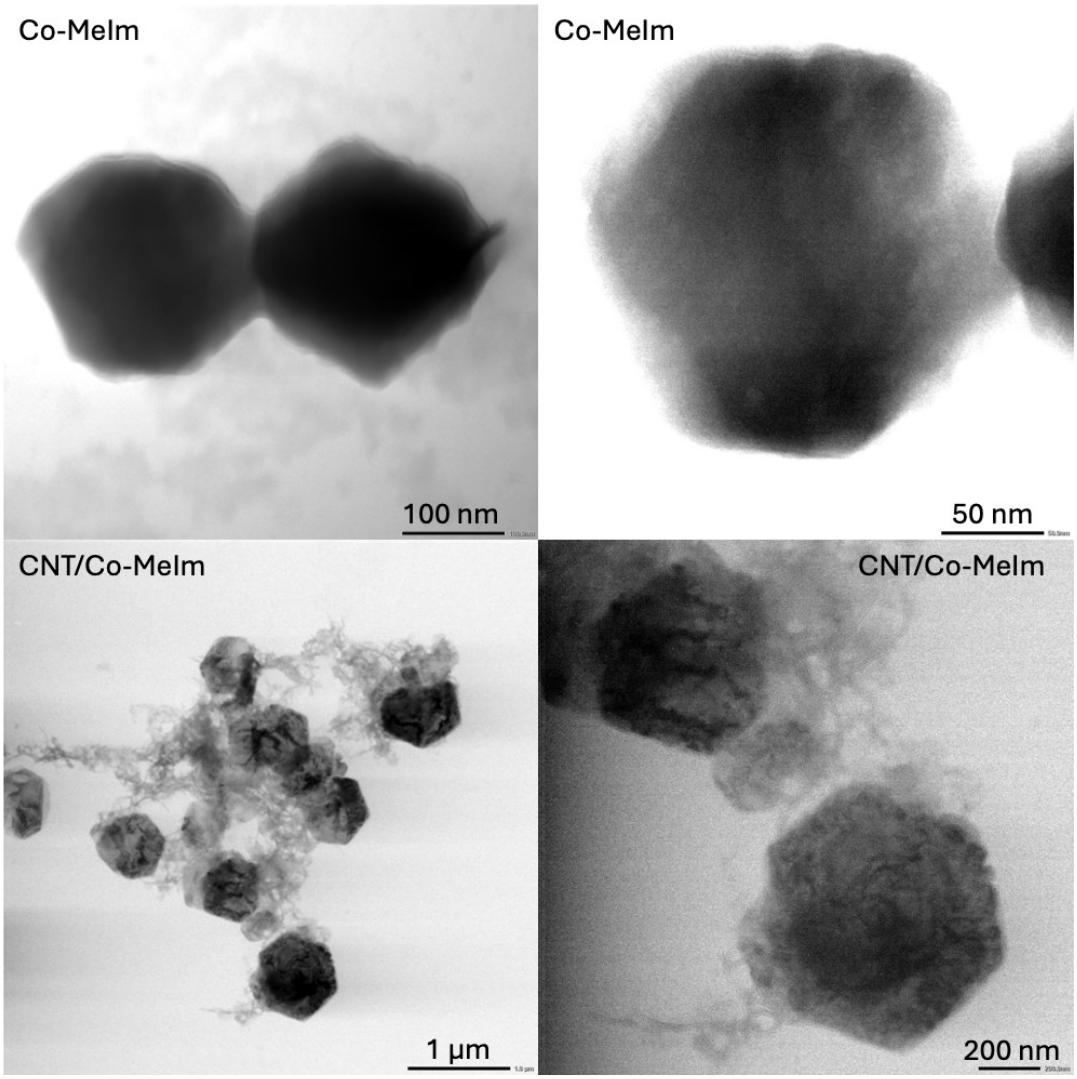

Fig. S2. TEM image of Co-MeIm and CNT/Co-MeIm show that some of CNTs are encapsulated inside the Co-MeIm crystal

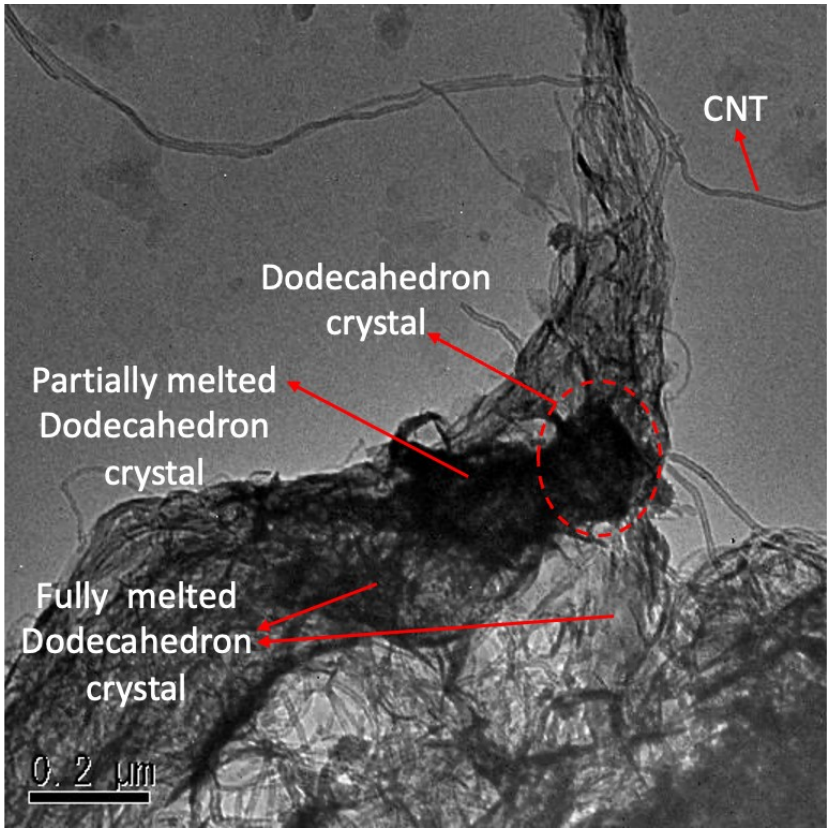

Fig. S3. TEM image of CNT/Co-MeIm-NQSO that capture crystal transformations among the CNTs networks

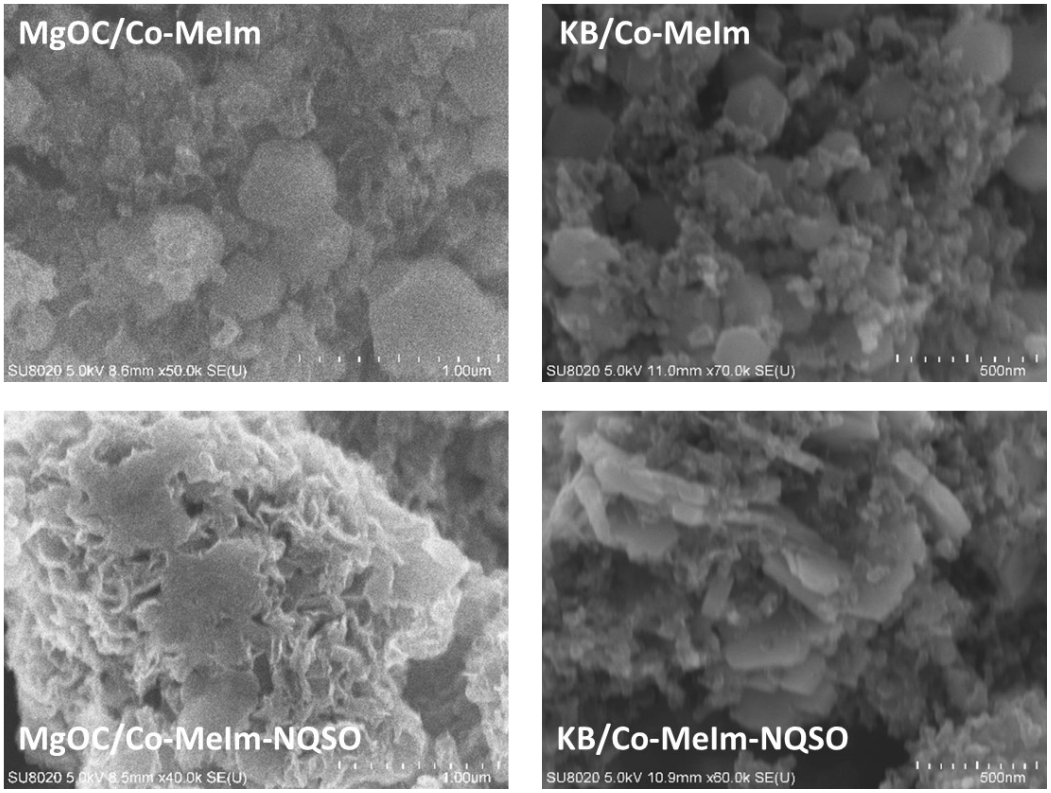

Fig. S4. SEM images of Co-Meim modified porous carbon (MgOC) and ketjen black (KB) before and after NQSO ligand substitution

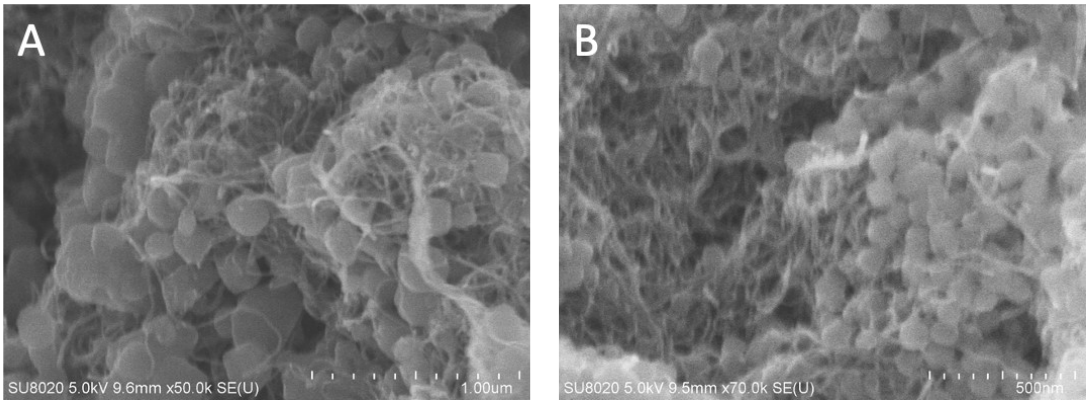

Fig. S5. SEM images of A. CNT/Co-MeIm-NQ and B. CNT/Zn-MeIm-NQSO

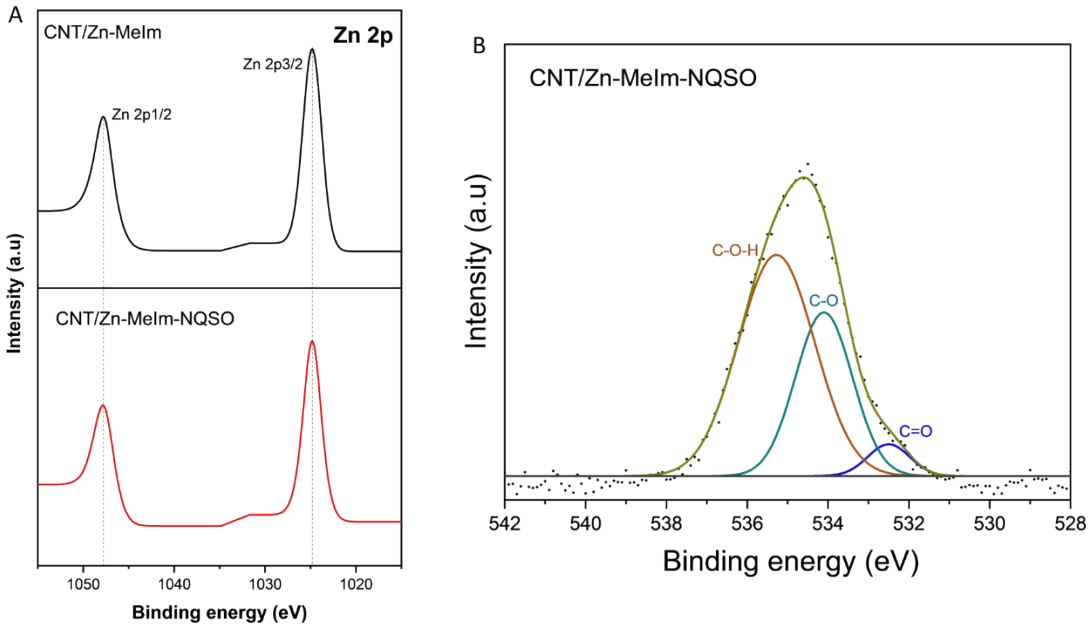

Fig. S6. XPS spectra of CNT/Zn-MeIm and CNT/Zn-MeIm-NQSO; A. at Zn 2p region and B. at O1s region

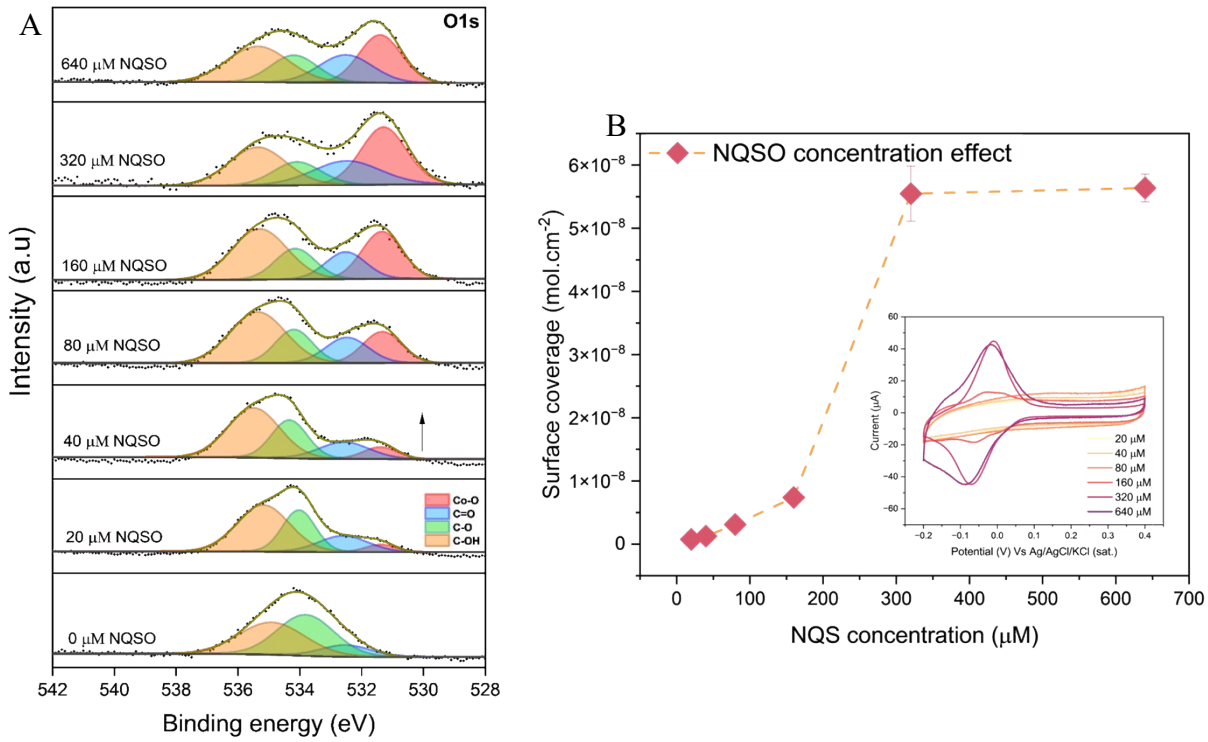

Fig. S7. A. XPS spectra of CNT/Co-MeIm-NQSO at O1s region toward the increment NQSO concentration during the ligand substitution process. B. The effect of NQSO concentration towards its surface coverage in CNT/Co–MeIm–NQSO, evaluated based on the CV in 0.1 M PBS at 5 $mV \cdot s^{-1}$ as in the inset figure

Supplementary S2 : Electron diffusion calculation

Electron diffusion coefficient D_{ex} was calculated as follows:

$$D_{ex} = k_b C_m \delta^2/6$$

Where ;

k_b :*electron exchange rate constant of* 1,2 – *Naphtoquinone* – 4 – *Sulfonate* $(3.98\ x\ 10^6\ M^{-1}S^{-1})$ [5]

C_m : *Concentration of redox active site in CNT/Co* – *MeIm* – *NQSO* (M)

which can be calculated as follows :

$$C_m = \frac{moles\ of\ redox\ sites\ (NQSO)}{V(cm^3)} \sim \frac{Surface\ coverage\ of\ NQSO\ (mol.cm^{-2})}{Thickness\ of\ redox\ active\ layer\ (cm)}$$

Thickness of redox active layer is obtained from cross sectional SEM wich is about $5\ x\ 10^{-4}$ *cm*

Hence :

$$C_m = \frac{5.54\ \times\ 10^{-8}\ mol.cm^{-2}}{5\ x\ 10^{-4}\ cm} = 0.1108\ M$$

And

δ :*Is the distance between adjecent NQSO sites* $(4.24\ \text{Å}\ or\ 4.24x10^{-8}\ cm)$

which is aproximately to be equal to the distance of Co to Co in the frameworks

Finally the D_{ex} *can be calculated*

$$D_{ex} = \frac{3.98\ x\ 10^6\ M^{-1}S^{-1}\ x\ 0.1108\ M\ x\ (4.24x10^{-8}\ cm)^2}{6}$$

$D_{ex=}\ 1.32\ x\ 10^{-10}\ cm^2.S^{-1}$

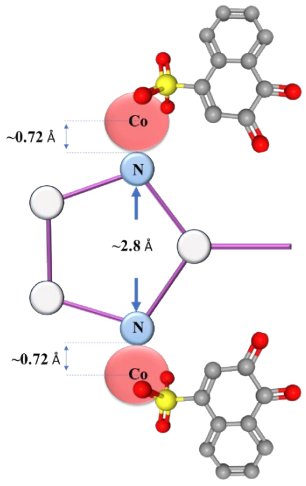

Table S1. Electron diffusion coefficient comparison

Embedded mediators	Electron diffusion coefficient (cm^2/s)	Ref
Ferrocene-Modified Poly (ethylene glycol)	9.1×10^{-12}	6
Electropolymerized Methylene Blue	3.7×10^{-13}	7
Poly (vinyl ferrocene)	2.6×10^{-10}	8
10-methyl1,3-vinyl phenothiazine	3.2×10^{-11}	9
NQ-LPEI	1.26×10^{-11}	10
CNT/Co-MeIm-NQSO	1.32×10^{-10}	This work

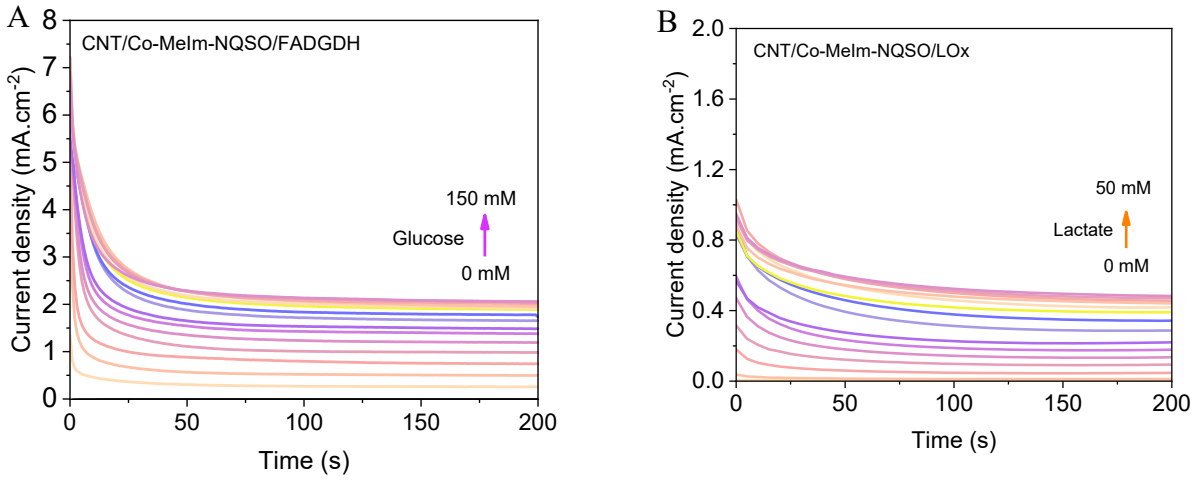

Fig. S8. A. CNT/Co-MeIm/FADGDH-electrode response toward the serial addition of glucose. B. CNT/Co-MeIm/LOx-electrode response toward the serial addition of lactate. Measurements were conducted at constant applied voltage of 0.3V

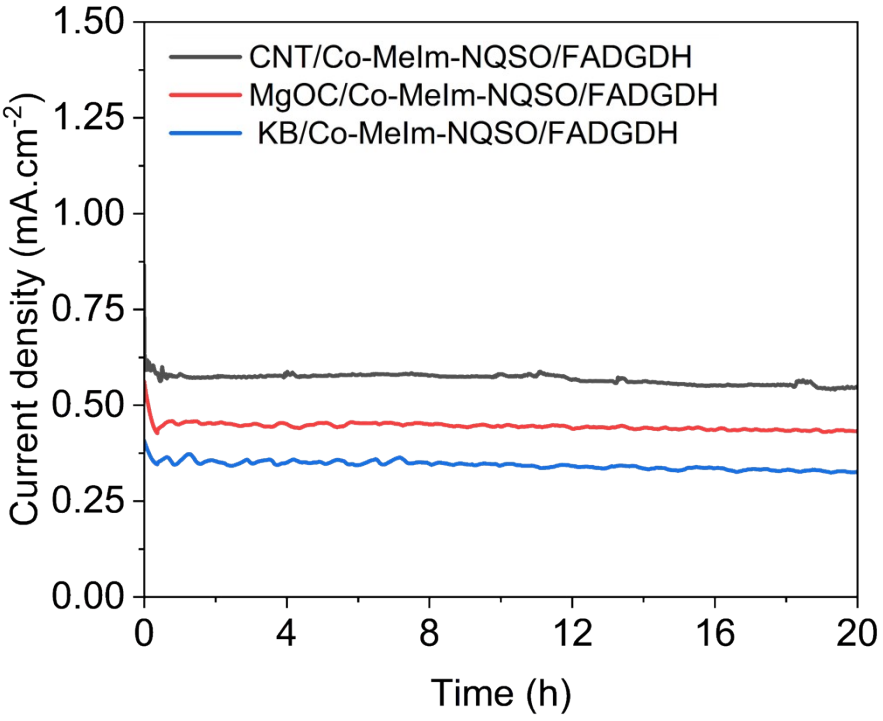

Fig. S9. CA measurement in 25 mM glucose of CNT/Co-MeIm-NQSO, MgOC/Co-MeIm-NQSO, and KB/Co-MeIm-NQSO, modified FADGDH.

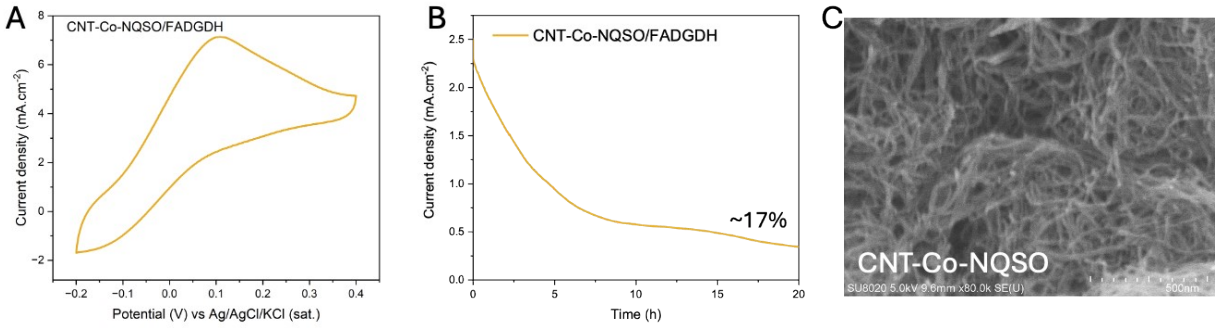

Fig. S10. A. CV measurement of CNT-Co-NQSO/FADGDH in 100 mM glucose (scan rates 25 mV.s-1), B. CA measurement of CNT-Co-NQSO/FADGDH in 100 mM at 0.3 V, and C. SEM image of CNT-Co-NQSO

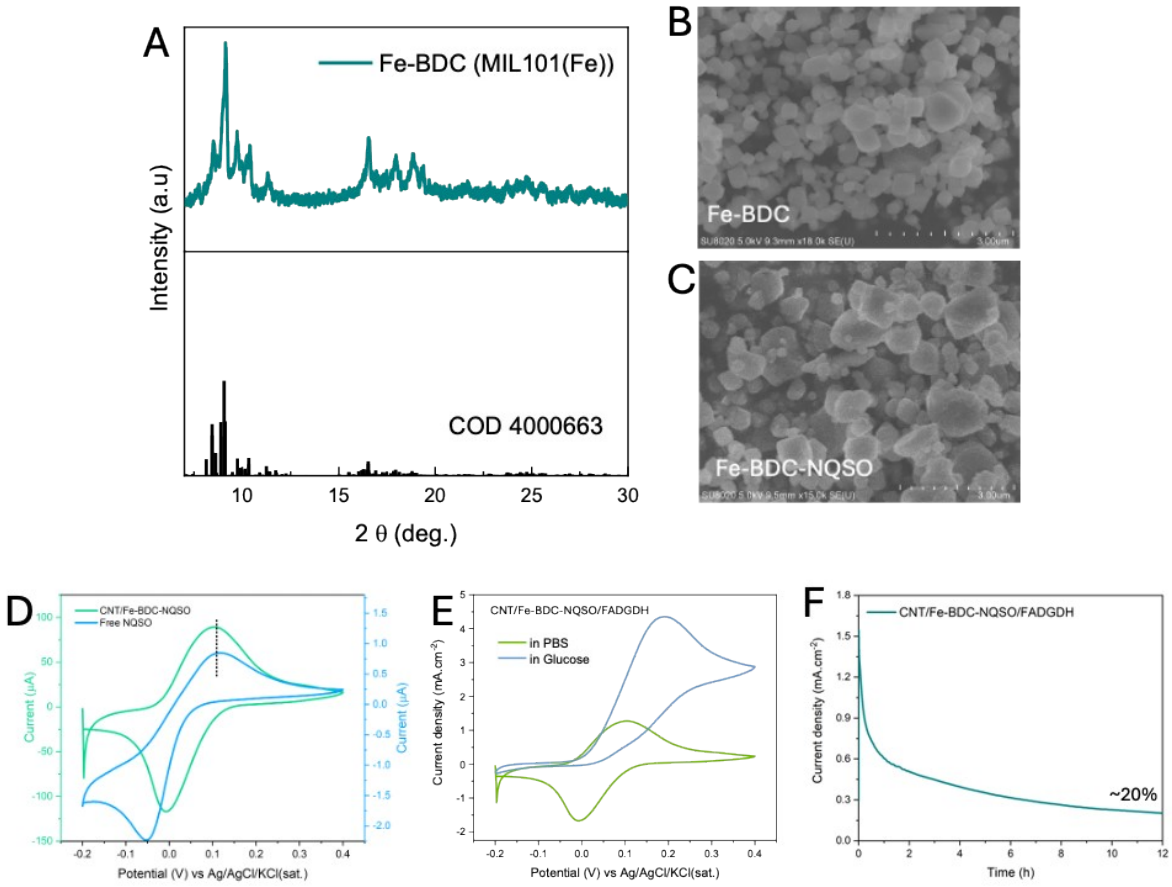

Fig. S11. A. XRD pattern of the synthesized Fe-BDC and its comparison with crystallography open data base (COD) 4000663 [11], B. SEM images of Fe-BDC and C. Fe-BDC-NQSO, D CV measurement in 0.1 M PBS that shows a similar peak position of CNT/Fe-BDC-NQSO and free NQSO, E. CV curve of CNT/Fe-BDC-NQSO modified FADGDH in the absence and the presence of 100 mM glucose (scan rates : 5 $mV.s^{-1}$) and F. the chrono amperometry measurement of CNT/Fe-BDC-NQSO/FADGDH in 100 mM glucose at applied voltage of 0.3V.

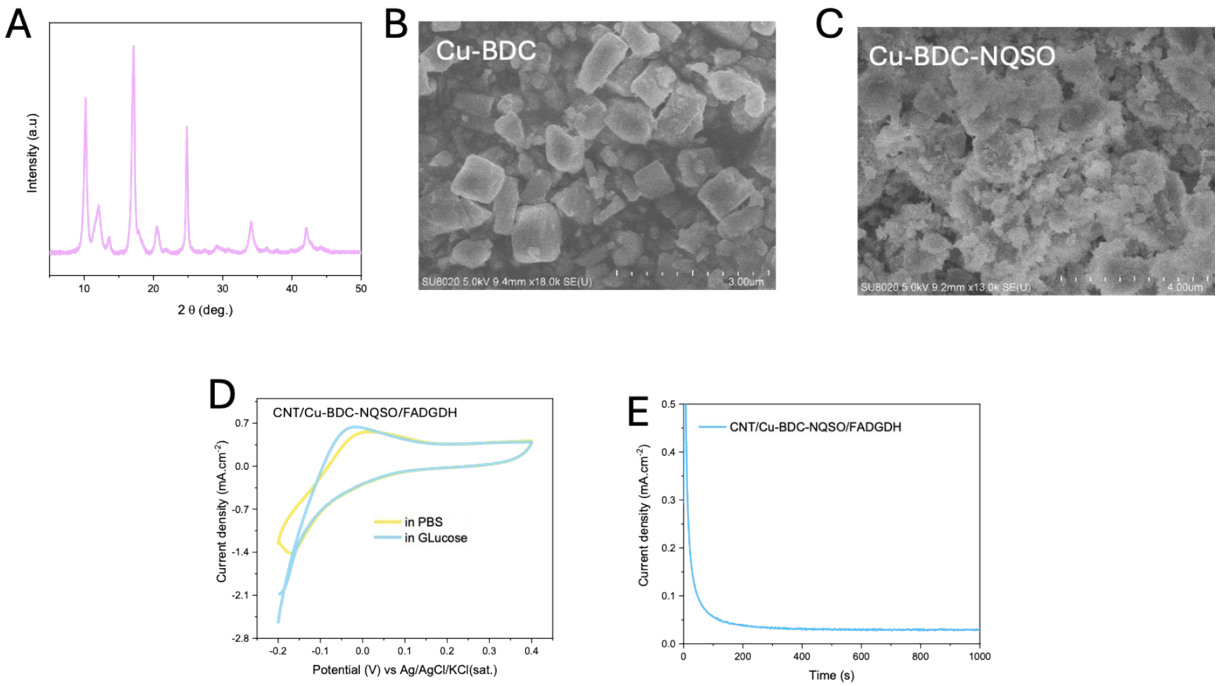

Fig. S12. A. XRD pattern of the synthesized Cu-BDC, B. SEM image of Cu-BDC, and C.SEM image of Cu-BDC-NQSO, D. CV of CNT/Cu-BDC-NQSO/FADGDH in PBS and in 100 mM glucose (5 $mV.s^{-1}$ of scan rates), and E. CA measurement of CNT/Cu-BDC-NQSO/FADGDH in 100 mM glucose.

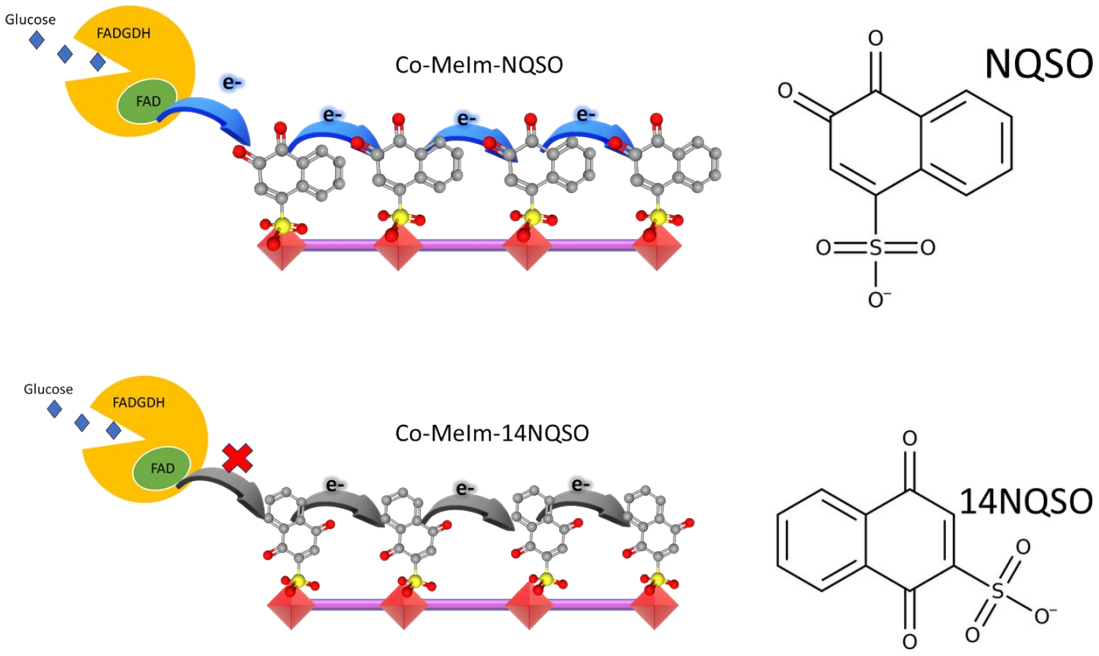

Fig. S13. Naphthoquinone site orientation in the raMOF toward the ability of Enzyme MET

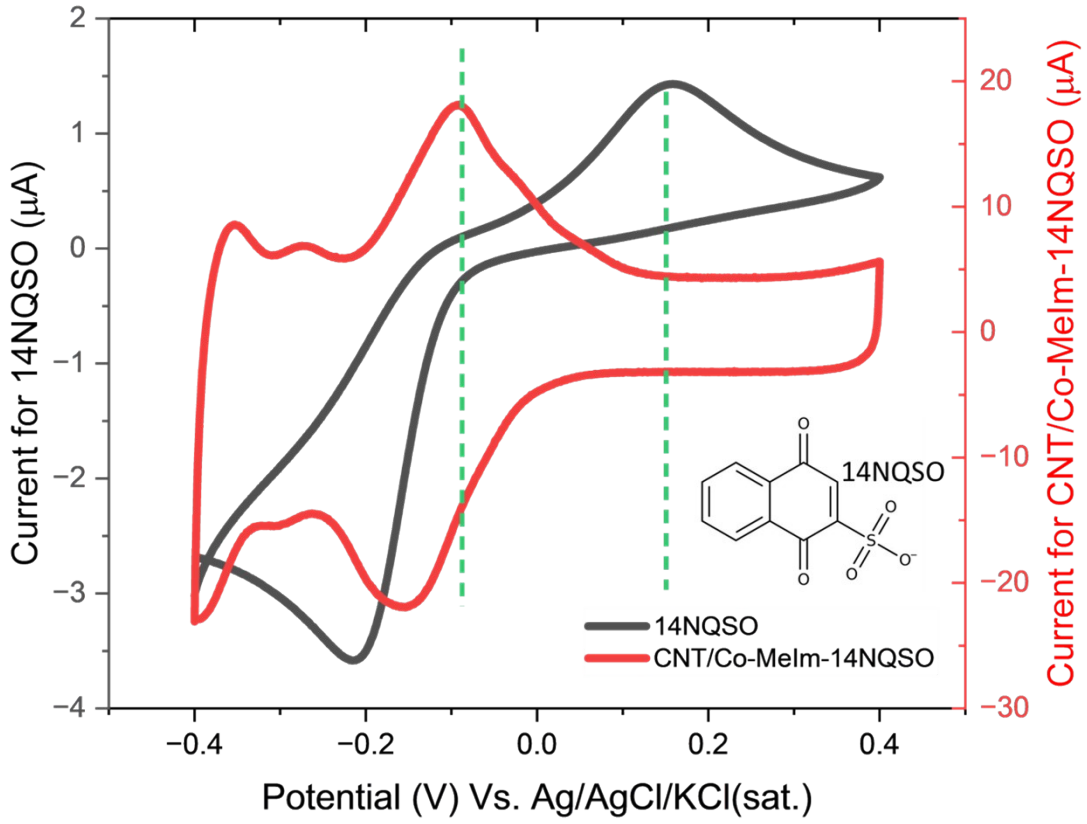

Fig. S14. A shift in the redox peak position of immobilized 14NQSO in Co-MeIm compared to its free form, measured in 0.1 M PBS, pH=7, scan rate of 5 $mV.s^{-1}$

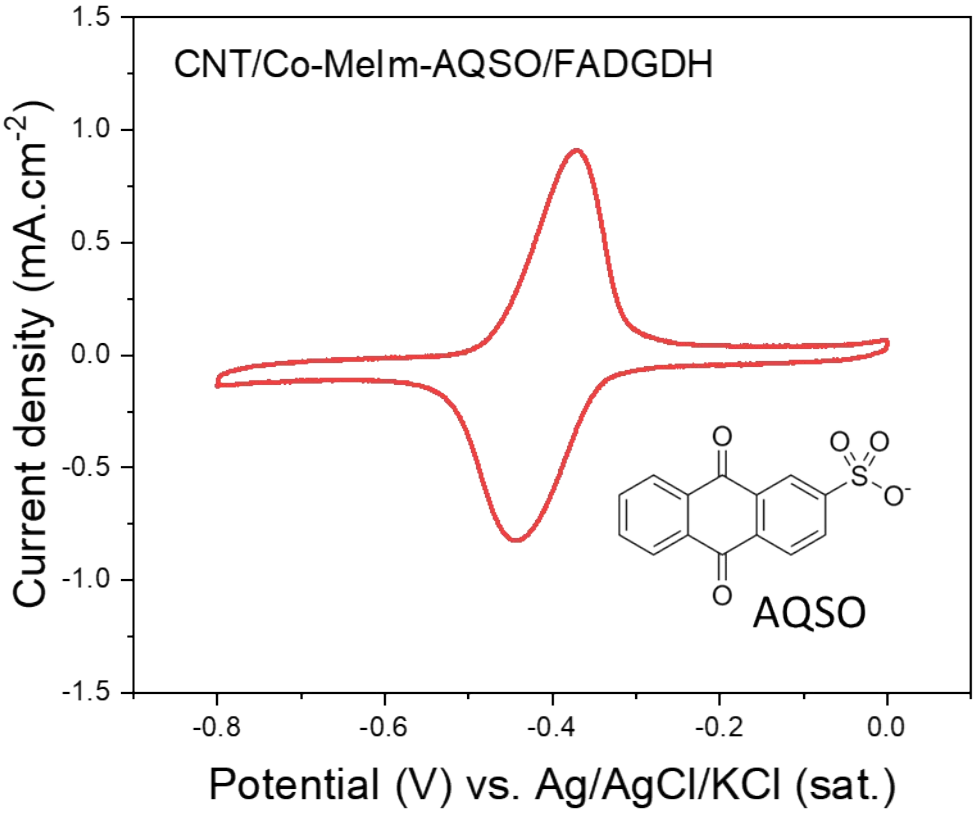

Fig. S15. CV of CNT/Co-MeIm-AQSO/FADGDH modified electrode in 100 mM glucose

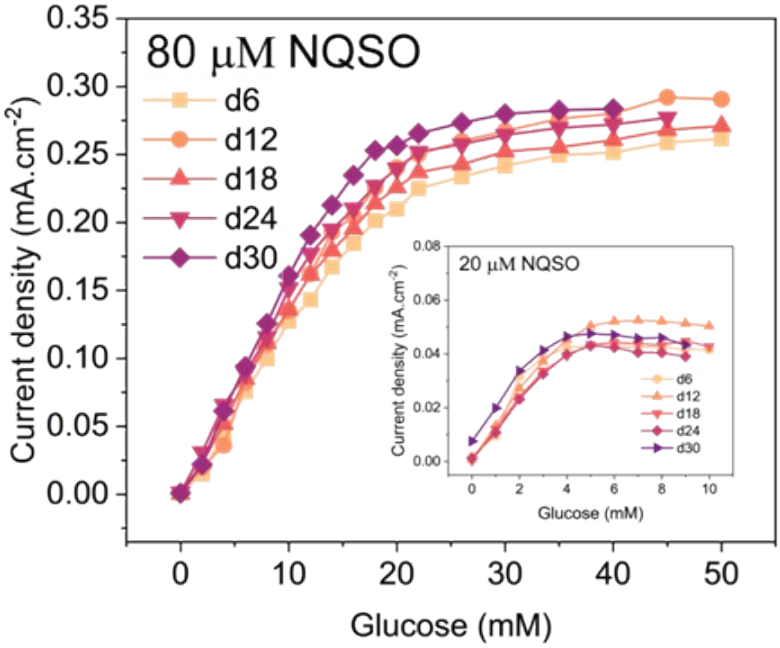

Fig. S16. Stability of the linear response range of the enzyme electrode based on CNT/Co-MeIm-NQSO/ FADGDH over 30 days of storage, with periodic measurements (the electrode was stored at 4°C in buffer when not in use).

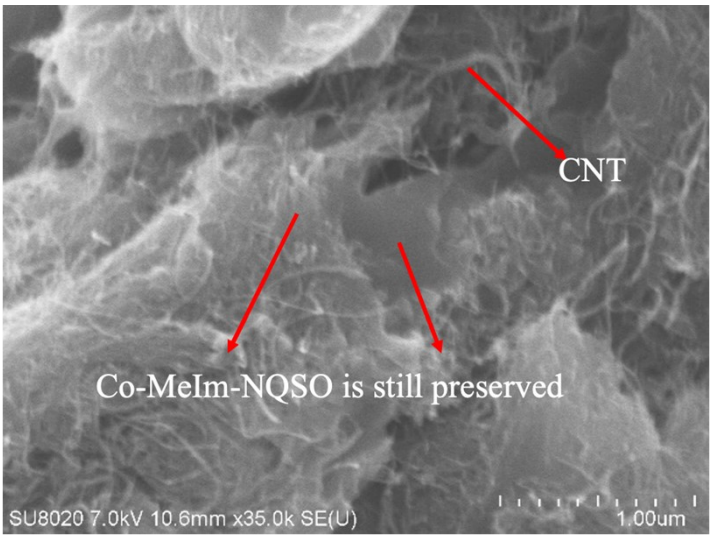

Fig. S17. SEM image after 54 h continuous enzymatic reaction in 20 mM glucose (pH=7)

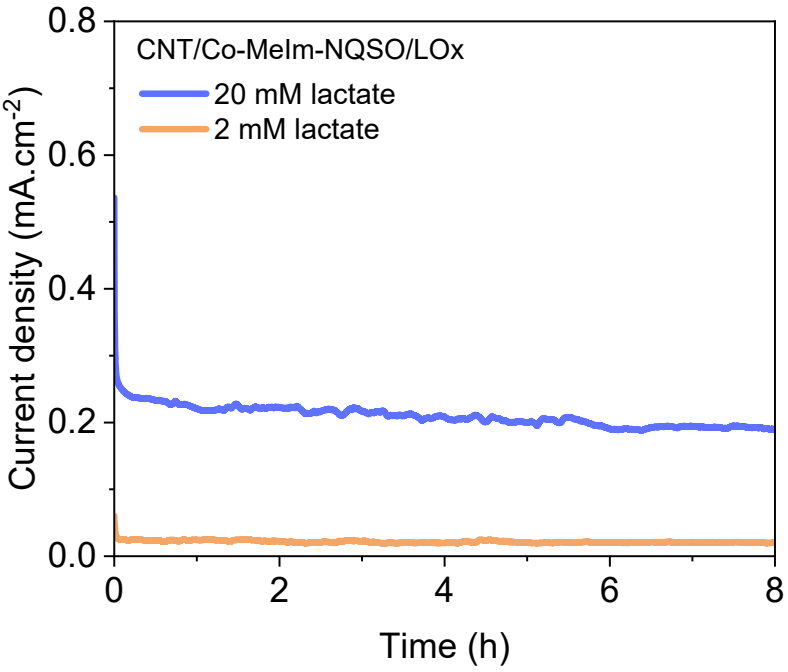

Fig. S18. Continuous CA measurements of CNT/Co-MeIm-NQSO/LOx electrode in the presence of 20 mM and 2 mM lactate at the constant applied voltage of 0.3V

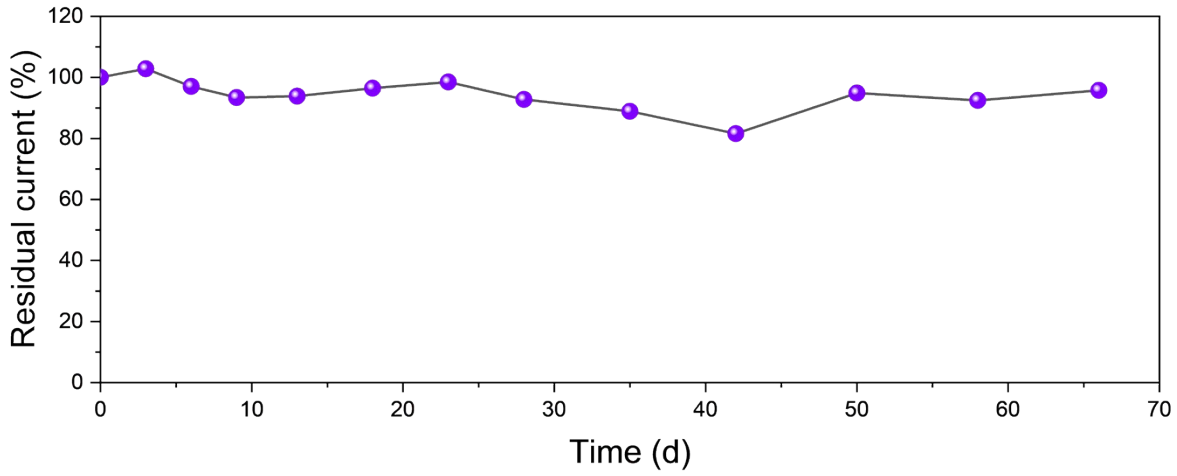

Fig. S19. Storage stability test of the CNT/Co-MeIm-NQSO/FADGDH electrode with periodic measurements over 66 days. The electrode was stored in PBS at 4°C when not in use

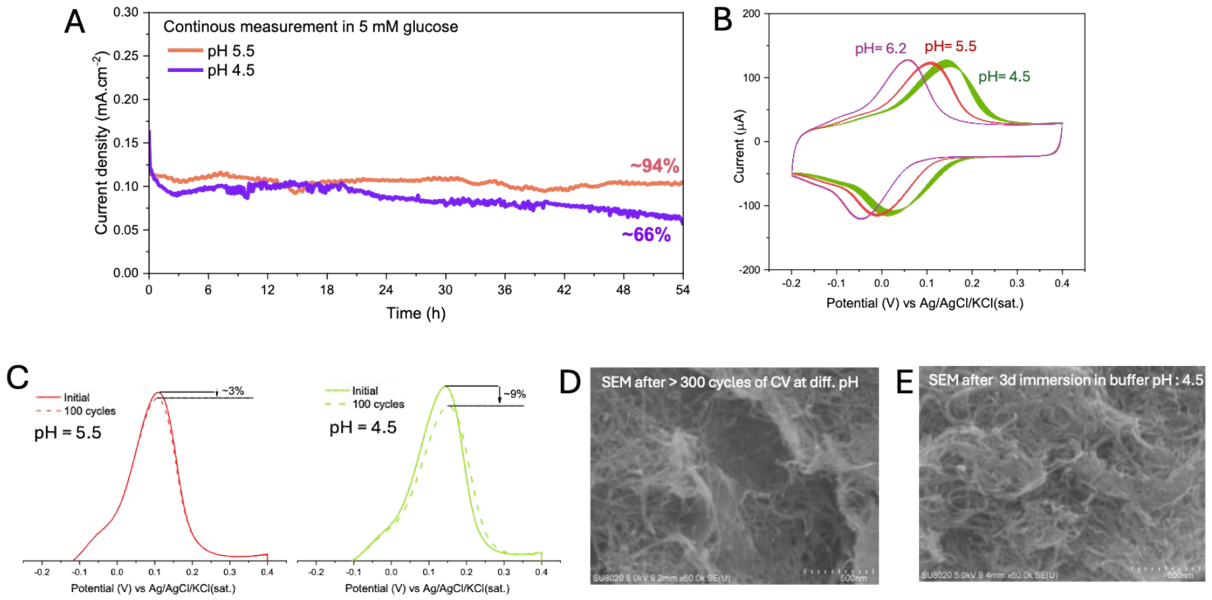

Fig. S20. A. CA measurement of the CNT/Co-MeIm-NQSO/FADGDH electrode in 5 mM glucose at pH 5.5 and pH 4.5.B. CV measurement for 100 cycles of the CNT/Co-MeIm-NQSO electrode at different pH levels: 6.2, 5.5, and 4.5. C. Comparison of oxidation peaks before and after 100 CV cycles at pH 5.5 and pH 4.5. D. SEM images of the CNT/Co-MeIm-NQSO electrode after more than 300 CV cycles at pH 6.2, pH 5.5, and pH 4.5. E. SEM image of the CNT/Co-MeIm-NQSO electrode after 3 days of immersion in buffer at pH 4.5

Table S2. Performance of nanostructured raMOF based enzyme electrode compared to previous reported works.

Material	Enzyme	Mediator	Analyte	Mediator immobilization Technique	J max ($mA.cm^{-2}$)	Continuous operation / stability	Ref
MWCNT/Pyr-NQ/PQQ-GDH	PQQ-GDH	Naphthoquinone	Glucose	Phi-phi interaction	0.1662	~	[12]
MWCNT/Os-(dmbpy)PVI-PEGDGE-FADGDH	FADGDH	Os-(dmbpy)PVI	Glucose	Redox polymer	2.7	20 h / 40%	[13]
BP-phyrene-NHS-Thionine /FADGDH	FADGDH	Thionine	Glucose	Surface modification-covalent bond	1.98	~	[14]
GCE/NQ-4-LPEI/FADGDH	FADGDH	Naphthoquinone	Glucose	Redox polymer	1.95	~	[10]
CNT/4-NBA/[Chit/GOx/ GP/GOx]	GOx	nitrobenzoic acid	Glucose	Surface absorption	0.331	~	[15]
MWCNT/DCNQ/FADGDH	FADGDH	Naphthoquinone	Glucose	Surface absorption	0.55	14 h/ 78%	[16]
GCE/ PEI-CNNQ/FADGDH	FADGDH	Naphthoquinone	Glucose	Redox polymer	1.97	15 h/34%	[17]
CNT-AAdiaz/FADGDH	FADGDH	Azure A	Glucose	Electro grafting	2.0	~	[18]
Thionine-FADGDH-PEGDGE	FADGDH	Thionine	Glucose	Crosslinking	0.4	10 h/5%	[19]
Thionine-FADGDH-NHS	FADGDH	Thionine	Glucose	Crosslinking	0.83	10 h/15%	[20]
Dicyano viologen-polymer/FADGDH	FADGDH	Dicyano viologen	Glucose	Redox polymer	0.053	~	[21]
CNT/Co-MeIm-NQSO/FADGDH	FADDGH	Naphthoquinone	Glucose	raMOF	2.06	54 h/100%,	This work
CNT/TTF/Cs-LOx + membrane	LOx	Tetrathiafulvalene	Lactate	Surface absorption	0.15	~	[22]
LOx-hexahistidine-phebazine	LOx	Phenazine	Lactate	Crosslinking	0.03	2h	[23]
LOx-PEGDGE- Phenazine	LOx	Phenazine	Lactate	Crosslinking	0.013	~	[24]
CNT/TTF/BSA-Cs-LOx	LOx	Tetrathiafulvalene	Lactate	Surface absorption	0.26	8 h	[25]
CNT/Co-MeIm-NQSO/LOx	LOx	Naphthoquinone	Lactate	raMOF	0.48	8 h/88%	This work

References

1 A. D. S. Barbosa, D. Julião, D. M. Fernandes, A. F. Peixoto, C. Freire, B. de Castro, C. M. Granadeiro, S. S. Balula and L. Cunha-Silva, *Polyhedron*, 2017, **127**, 464–470.

2 H. R. Mahdipoor, R. Halladj, E. Ganji Babakhani, S. Amjad-Iranagh and J. Sadeghzadeh Ahari, *RSC Adv.*, 2021, **11**, 5192–5203.

3 M. Rezki, N. L. W. Septiani, M. Iqbal, S. Harimurti, P. Sambegoro, D. R. Adhika and B. Yuliarto, *J Mater Chem B*, 2021, **9**, 5711–5721.

4 K. Zhou, B. Mousavi, Z. Luo, S. Phatanasri, S. Chaemchuen and F. Verpoort, *J. Mater. Chem. A*, 2017, **5**, 952–957.

5 N. Tsuruoka, T. Sadakane, R. Hayashi and S. Tsujimura, *Int J Mol Sci*, DOI:10.3390/ijms18030604.

6 T. Steentjes, P. Jonkheijm and J. Huskens, *Langmuir*, 2017, **33**, 11878–11883.

7 T. Komura, G. Y. Niu, T. Yamaguchi, M. Asano and A. Matsuda, *Electroanalysis*, 2004, **16**, 1791–1800.

8 G. Inzelt and L. Szabo, *Electrochim Acta*, 1986, **31**, 1381–1387.

9 H. Nagasaka and M. Watanabe, *Polym Adv Technol*, 1995, **6**, 190–196.

10 R. D. Milton, D. P. Hickey, S. Abdellaoui, K. Lim, F. Wu, B. Tan and S. D. Minteer, *Chem Sci*, 2015, **6**, 4867–4875.

11 O. I. Lebedev, F. Millange, C. Serre, G. Van Tendeloo and G. Férey, *Chemistry of Materials*, 2005, **17**, 6525–6527.

12 F. Giroud, R. D. Milton, B.-X. Tan and S. D. Minteer, *ACS Catal*, 2015, **5**, 1240–1244.

13 I. Osadebe and D. Leech, *ChemElectroChem*, 2014, **1**, 1988–1993.

14 L. Fritea, A. J. Gross, K. Gorgy, R. K. O'Reilly, A. Le Goff and S. Cosnier, *J. Mater. Chem. A*, 2019, **7**, 1447–1450.

15 K. Hyun, S. Kang, J. Kim and Y. Kwon, *ACS Appl Mater Interfaces*, 2020, **12**, 23635–23643.

16 R. Cohen, R. E. Bitton, N. S. Herzallh, Y. Cohen and O. Yehezkeli, *Anal Chem*, 2021, **93**, 11585–11591.

17 C. Hou, Q. Lang and A. Liu, *Electrochim Acta*, 2016, **211**, 663–670.

18 A. J. Gross, S. Tanaka, C. Colomies, F. Giroud, Y. Nishina, S. Cosnier, S. Tsujimura and M. Holzinger, *ChemElectroChem*, 2020, **7**, 4543–4549.

19 M. M. Hossain, J. Morshed and S. Tsujimura, *Chemical Communications*, 2021, **57**, 6999–7002.

20 M. M. Hossain, M. Rezki, I. Shalayel, A. Zebda and S. Tsujimura, *ACS Appl Mater Interfaces*, 2024, **16**, 44004–44017.

21 S. Chandra, A. Lielpetere and W. Schuhmann, *Sens Actuators B Chem*, 2023, **397**, 134660.

22 A. M. Zamarayeva, N. A. D. Yamamoto, A. Toor, M. E. Payne, C. Woods, V. I. Pister, Y. Khan, J. W. Evans and A. C. Arias, *American Institute of Physics Inc.*, 2020, preprint, DOI: 10.1063/5.0014836.

23 Q. He, C. Wang, R. Jain, J. Byrnes, E. R. Farquhar, E. Reed, E. Berezovsky, M. R. Chance, D. Lodowski and R. An, *Heliyon*, 2024, **10**, e34301.

24 K. Hiraka, K. Kojima, W. Tsugawa, R. Asano, K. Ikebukuro and K. Sode, *Biosens Bioelectron*, 2020, **151**, 111974.

25 W. Jia, A. J. Bandodkar, G. Valdés-Ramírez, J. R. Windmiller, Z. Yang, J. Ramírez, G. Chan and J. Wang, *Anal Chem*, 2013, **85**, 6553–6560.